

A Class of Nonplanar Conjugated Compounds with Aggregation-Induced Emission: Structural and Optical Properties of 2,5-Diphenyl-1,4-distyrylbenzene Derivatives with All Cis Double Bonds

Zengqi Xie, Bing Yang, Weijie Xie, Linlin Liu, Fangzhong Shen, Huan Wang, Xuyan Yang, Zhiming Wang, Yupeng Li, Muddasir Hanif, Guangdi Yang, Ling Ye, and Yuguang Ma*

Key Laboratory for Supramolecular Structure and Materials of Ministry of Education, Jilin University, Changchun, 130012, P. R. China

Received: June 29, 2006; In Final Form: August 17, 2006

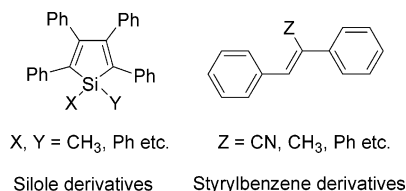
We have studied the structural and optical properties of four 2,5-diphenyl-1,4-distyrylbenzene derivatives with all cis double bonds. These compounds belong to a class of nonplanar conjugated compounds possessing a typical Aggregation-Induced Emission (AIE) property that has no emission in solution but intense emission in crystal. The four molecules are packed in different stacking modes with different intermolecular interactions, resulting in different crystalline state photoluminescence (PL) efficiency. The torsional molecular configuration increases the intermolecular distances effectively in the crystalline state, which decreases the difference of the optical properties from the frozen isolated molecules to the crystalline state. The Stokes shifts of these compounds are very large and the PL spectra have only one broad emission band with poor structure, due to the relatively large configuration difference between the ground state and the first singlet excited state, and the abundant vibration energy levels of the torsional molecule with changeable conformation.

Introduction

Many conjugated organic luminescent materials have very high luminescence efficiency in their dilute solutions, but they exhibit relatively weak emission when fabricated into thin films, due to the formation of less emissive species such as excimers in the aggregate state.¹ It is especially significant in obtaining high solid-state luminescence efficiency, for the devices, e.g., organic light-emitting diodes (OLEDs) and lasers, just work in film or the crystalline state. Thus increasing attention has been paid to enhance the solid-state luminescence efficiency by using chemical, physical, and engineering approaches, with limited success.² Aggregation in some sense is inherent in film formation, and it would be an ideal case if a molecule can emit intense light in its aggregate state.

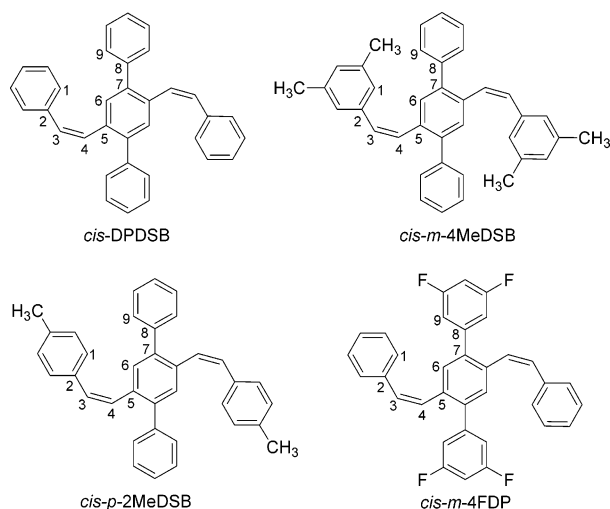
In the past few years, materials with aggregation-induced emission (AIE) properties have attracted more and more attention, because they possess our desired property, the enhanced emission from the aggregate state. Up to now, enhanced emission due to aggregation has been reported for silole derivatives and styrylbenzene derivatives. Since the first AIE active material 1-methyl-1,2,3,4,5-pentaphenylsilole³ was reported by Tang's group, many silole derivatives have been synthesized, such as 1,1-bis(2'-thienyl)-2,3,4,5-tetraphenylsilole⁴ and silole containing polymers.⁵ Earlier, it was believed that the AIE phenomenon was due to the effects of intramolecular planarization in the solid state, supported by the increase in the absorbance.³ However, later studies on the crystals of silole derivatives revealed that their twisted configurations are maintained in the solid state, and suggested that the restricted intramolecular vibrational and rotational motions in the solid state cause the AIE phenomenon based on the effects of viscosity and temperature on the emission behaviors.⁶ This proposal is also

supported by the synthesis of substituted siloles,⁷ time-resolved technique,⁸ and calculation results.⁹



As for styrylbenzene derivatives, the reported AIE active materials include CN-MBE,¹⁰ NPAFN,¹¹ PPB,¹² TPBD,¹³ conjugated polymers,¹⁴ and others.¹⁵ All of them have substituents on the double bonds, such as cyano, methyl, and phenyl groups, which make the backbone deviate from a conjugated plane. Several models, such as exciton diffusion, coplanarization, and stabilized excited state, have been proposed for the enhanced emission in the solid state of such types of materials. In the diphenyl-substituted PPV system,^{14b} Belton et al. explained that in the solid state the rigid packing produces severe torsional hindrances along the polymer backbone, which results in large energy barriers to exciton hopping along the chain and prevents exciton diffusion to quenching sites, and then raises the photoluminescence (PL) yield. Park et al.^{10a} proposed that the twisted structure is responsible for the PL quenching of CN-MBE in solution, while coplanarization in the solid state caused their AIE. But recent research on the crystal structure of PPB indicates that the ethene moieties are twisted with respect to the benzene rings with an average torsional angle of 31° maintained in the crystal.¹² Fluorescence transients of PPB on a femtosecond scale indicate an efficient channel for isomerization that is activated for free PPB in solution but inhibited in PPB forming nanoparticles, demonstrating the significance of molecular geometry and twisting motions that affect the relaxation dynamics in the excited state.

* Address correspondence to this author. E-mail: ygma@jlu.edu.cn.

CHART 1: Chemical Structures of 2,5-Diphenyl-1,4-distyrylbenzene Derivatives with All Cis Double Bonds


Comparing the molecular structure and luminescence properties of the AIE active materials, we can find the commonality is that all the chromophores have a twisted conformation, and most of the emission spectra of these materials have only one emission peak with poor structure. Study on the intrinsic luminescence properties of such types of nonplanar conjugated compounds may help us to design novel luminescent materials with high solid-state luminescence efficiency.

Recently we have synthesized a nonplanar molecule *cis*-DPDSB (2,5-diphenyl-1,4-distyrylbenzene with two *cis* double bonds), which has large torsional angles along both the distyrylbenzene direction and the *p*-terphenyl direction.¹⁶ It is well-known that the *cis*-vinylene generally shows weak luminescence and was regarded as “*cis*-defect” in poly(*p*-phenylene vinylene)s (PPVs).¹⁷ Our research indicates that *cis*-DPDSB shows very intense blue emission in the crystalline state, although there is almost no emission in molecularly dissolved solutions. The very weak emission in solution is caused by photochemical processes: *cis*-trans isomerization and photocyclization resulting from or together with intramolecular vibrational and rotational motions of the double bonds.¹⁶ The intense emission from the crystal of *cis*-DPDSB probably can be attributed to the stabilized excited state due to the supramolecular interactions.¹⁶ But the photophysical properties, such as very large Stokes shift (~120 nm) and structureless emission spectrum, are very unique when compared with most of the PPV-type materials.¹⁸ Our present work is to find out the essential emission species in the crystals of the *cis* isomers and the reasons for their unique emission properties.

We have designed and synthesized four *cis*-2,5-diphenyl-1,4-distyrylbenzene derivatives (Chart 1). The minor modification of the molecular structures is to induce different stacking modes, which is helpful in understanding the effect of the stacking mode on the optical properties such as aggregate-particles absorption properties and crystalline state PL efficiency. The frozen dilute chloroform solution of the *cis* isomers glass state is used to record the emission properties of the isolated *cis* isomers. Herein, we report the results.

Experimental Section

THF was purified by fractional distillation before use as solvent. The four *cis* compounds with different substituents were synthesized by Wittig reaction, and were fully characterized by

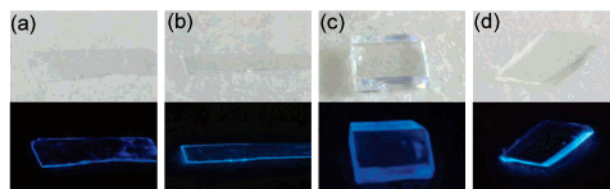


Figure 1. Photographs of the crystals of (a) *cis*-DPDSB, (b) *cis*-*m*-4MeDSB, (c) *cis*-*p*-2MeDSB, and (d) *cis*-*m*-4FDP under natural light (top) and UV light (bottom).

¹H NMR, FT-IR, elemental analysis, MALDI-TOF-MS, and differential scanning calorimetry (DSC) as described in ESI.

X-ray Crystallography. Single crystals of all the *cis* compounds were prepared by vaporizing mixed solvents of chloroform and methanol (1: 2) slowly at room temperature under rigorous exclusion of light. The diffraction experiments were carried out on a Rigaku R-Axis RAPID diffractometer equipped with Mo K α and Control Software using the RAPID AUTO at 293(±2) °C. Empirical absorption corrections were applied automatically. The structures were solved with direct methods and refined with a full-matrix least-squares technique, using the SHELXS v. 5.1 programs,¹⁹ respectively. The space groups were determined from the systematic absences and their correctness was confirmed by successful solution and refinement of structures. Anisotropic thermal parameters were refined for all the non-hydrogen atoms. The hydrogen atoms were located from difference maps and refined with isotropic displacement. Crystallographic data for the structures reported in this paper are in CIF files and have been deposited into the Cambridge Crystallographic Data Center as supplementary publication numbers CCDC 285922, 287320, 612746, and 612747. See <http://www.ccdc.cam.ac.uk>.

UV–vis absorption spectra were recorded on a UV-3100 spectrophotometer. Fluorescence measurements were carried out with RF-5301PC. Crystalline state PL efficiencies were measured with an integrating sphere.

Result and Discussion

The four compounds with all *cis* double bonds were synthesized utilizing a 2-fold Wittig reaction, and were fully characterized by NMR, FT-IR, elemental analysis, MALDI-TOF mass spectrum, and differential scanning calorimetry (DSC) methods as described in ESI. We prepared the single crystals for X-ray diffraction experiment by vaporizing mixed solvents of chloroform and methanol (1: 2) slowly at room temperature under rigorous exclusion of light. All of the four crystals are colorless with relatively good photochemical stability. After the crystals were exposed to irradiation of a high-pressure mercury-arc light source (125 W) in N₂ for 5 min, no color change was observed and there was no photoisomerization product trans isomer monitored by FT-IR. The growth habits are prisms (thin slices) for *cis*-DPDSB and *cis*-*m*-4MeDSB, and blocks for *cis*-*p*-2MeDSB and *cis*-*m*-4FDP (Figure 1). There are three conformational polymorphs for *cis*-DPDSB as discussed before,²⁰ but here we choose one of the most popular polymorph to compare with other compounds. The crystal data and structure refinements of four crystals are tabulated in Table 1.

Nonplanar Molecular Structures. Table 2 gives the selected dihedral and torsion angles of the four *cis* compounds in crystal structures. As we can see, in all four molecules, there are large torsions along both the distyrylbenzene direction and the *p*-terphenyl direction, which means the backbone of the *cis* isomer largely deviates from a plane and cofacial π – π stacking becomes impossible. The torsional angles of the double bonds

TABLE 1: Crystal Data and Structure Refinements of Four Crystals

| | <i>cis</i> -DPDSB | <i>cis</i> - <i>m</i> -4MeDSB | <i>cis</i> - <i>p</i> -2MeDSB | <i>cis</i> - <i>m</i> -4FDP |
|--|---------------------------------|---------------------------------|---------------------------------|--|
| empirical formula | C ₃₄ H ₂₆ | C ₃₈ H ₃₄ | C ₃₆ H ₃₀ | C ₃₄ H ₂₂ F ₄ |
| formula wt | 434.55 | 490.65 | 462.60 | 506.52 |
| <i>T</i> /K | 293(2) | 293(2) | 293(2) | 293(2) |
| crystal system | triclinic | monoclinic | monoclinic | triclinic |
| space group | <i>P</i> 1 | <i>P</i> 2(1)/ <i>c</i> | <i>P</i> 2(1)/ <i>n</i> | <i>P</i> 1 |
| <i>a</i> /Å | 5.4867(3) | 13.600(3) | 9.975(2) | 8.0544(16) |
| <i>b</i> /Å | 12.864(8) | 18.604(4) | 10.885(2) | 8.7247(17) |
| <i>c</i> /Å | 17.893(9) | 5.6750(11) | 25.805(5) | 10.764(2) |
| α /deg | 97.670(6) | 90 | 90 | 67.07(3) |
| β /deg | 90.915(1) | 90.36(3) | 98.23(3) | 88.05(3) |
| γ /deg | 96.004(3) | 90 | 90 | 66.99(3) |
| <i>V</i> /Å ³ | 1244.2(1) | 1435.9(5) | 2773.2(10) | 634.9(2) |
| <i>Z</i> | 2 | 2 | 4 | 1 |
| density/Mg/m ³ | 1.160 | 1.135 | 1.108 | 1.325 |
| μ (Mo K α)/mm ⁻¹ | 0.065 | 0.064 | 0.062 | 0.096 |
| θ range/deg | 1.15–27.48 | 3.00–27.48 | 1.59–27.48 | 3.02–27.47 |
| no. of reflns collected | 5280 | 13786 | 5934 | 6314 |
| no. of independent reflns | 5280 | 3281 | 5934 | 2880 |
| no. of reflns obsd | 1828 | 1851 | 1775 | 1613 |
| <i>R</i> (int) | 0.0000 | 0.0541 | 0.0000 | 0.0323 |
| GOF | 0.971 | 1.024 | 0.954 | 1.027 |
| <i>R</i> ₁ [<i>I</i> > 2 σ (<i>I</i>)] | 0.0646 | 0.0491 | 0.0657 | 0.0496 |
| <i>wR</i> ₂ [<i>I</i> > 2 σ (<i>I</i>)] | 0.0887 | 0.1099 | 0.1272 | 0.1043 |
| <i>R</i> ₁ (all data) | 0.2091 | 0.1012 | 0.2105 | 0.1018 |
| <i>wR</i> ₂ (all data) | 0.1086 | 0.1293 | 0.1467 | 0.1314 |

TABLE 2: Selected Dihedral and Torsion Angles (deg) in Crystal Structures of the Four Cis Compounds

| material | $\theta_{(1,2,3,4)}$ | $\theta_{(2,3,4,5)}$ | $\theta_{(3,4,5,6)}$ | $\theta_{(6,7,8,9)}$ |
|--|----------------------|----------------------|----------------------|----------------------|
| <i>cis</i> -DPDSB ^a | 43.5 | 7.4 | 36.7 | 49.6 |
| | 44.2 | 8.8 | 40.5 | 52.1 |
| <i>cis</i> - <i>m</i> -4MeDSB | 41.9 | 7.4 | 35.9 | 61.1 |
| <i>cis</i> - <i>p</i> -2MeDSB ^b | 46.0 | 6.1 | 37.6 | 44.7 |
| | 46.6 | 6.6 | 34.2 | 48.4 |
| <i>cis</i> - <i>m</i> -4FDP | 35.5 | 7.6 | 39.9 | 51.6 |

^a There are two crystallographically independent conformational molecules. ^b There is no symmetric center of the *cis*-*p*-2MeDSB molecule in the crystal.

and their adjacent phenyl rings ($\theta_{(2,3,4,5)}$) are distributed from 6° to 9°, and the torsional angle of its adjacent bonds ($\theta_{(1,2,3,4)}$ and $\theta_{(3,4,5,6)}$) is distributed from 34° to 47°. $\theta_{(2,3,4,5)}$ is obviously smaller than $\theta_{(1,2,3,4)}$ and $\theta_{(3,4,5,6)}$, which can be attributed to the effect of the π -electrons of the double bonds. Also the changeable torsional angles reflect that different stacking affects the molecular conformations more or less.

Molecular Stacking Features and Intermolecular Interactions. As shown in Figure 2a and Figure 3a, the molecules of *cis*-DPDSB and *cis*-*m*-4MeDSB are packed into molecular columns that are perpendicular to the plane of the central phenyl rings. The distances between two molecules within one column for *cis*-DPDSB and *cis*-*m*-4MeDSB are 5.49 (*d*₁) and 5.68 Å (*d*₂) respectively, which are too large to form the π - π interaction. Although *cis*-DPDSB and *cis*-*m*-4MeDSB are packed into different crystal systems with different space groups (for *cis*-DPDSB: crystal system, triclinic; space group, *P*1; for *cis*-*m*-4MeDSB: crystal system, monoclinic; space group, *P*2(1)/*c*), the stacking images are very similar except for different intermolecular distance.

There are two crystallographically independent conformational molecules in the crystal of *cis*-DPDSB. As shown in Figure 2b, there is an aromatic CH/ π hydrogen bond (interaction **I**) formed between two molecules with interaction distance of 3.09 Å, where the terminal phenyl ring along the distyrylbenzene segment of one molecule (drawn in green) acts as an H donor and the corresponding phenyl ring of the adjacent molecule (drawn in orange) acts as an H acceptor. This interaction may

help to hinder the rotation of the terminal phenyl ring on the distyrylbenzene segment. When the corresponding phenyl ring of the blue molecule is checked (interaction **II**), no aromatic CH/ π hydrogen bond is formed because of the very large distance (3.71 Å). Thus, only half of the total molecules in the crystal act as an H donor to form aromatic CH/ π hydrogen bonds. As for the crystal of *cis*-*m*-4MeDSB, the terminal phenyl ring on the distyrylbenzene segment acts as both an H donor and an H acceptor (interaction **III**, shown in Figure 3b). The interaction distance is relatively large (3.23 Å), which means the interaction is weak and has less effect on the rotation of this phenyl group.

The unit cell of *cis*-*p*-2MeDSB is monoclinic, space group *P*2(1)/*n*, containing four discrete asymmetric molecules. The asymmetric molecule indicates the presence of considerable packing forces in the crystal stacking. The molecules are packed layer-by-layer parallel to the (001) plane and the interlayer distance (*c*/2 sin β) is 12.77 Å. Within one layer, the molecules line into strings with head-to-tail image along the *b*-axis. The molecules between adjacent strings (in one layer) are packed into the simple “brickwall motif” in which each “brick”, or molecule, is situated over the gap between the bricks in the row below (Figure 4a).²¹ As for *cis*-*m*-4FDP, the molecule in the crystal is symmetric and packed into triclinic system with space group *P*1. Although it has the same crystal system and space group as *cis*-DPDSB, its packing mode is very similar to that of *cis*-*p*-2MeDSB (Figure 5a).

There are two kinds of aromatic CH/ π hydrogen bonds in the crystal of *cis*-*p*-2MeDSB as shown in Figure 4b (interactions **IV** and **V**), which enable the molecule to have asymmetric configuration. The central phenyl of each molecule acts as an H acceptor and the terminal phenyl rings of the distyrylbenzene segment act as H donors. The interaction distance and the angle of C–H– π center for interaction **IV** are 3.06 Å and 161.4°, and those for interaction **V** are 2.84 Å and 170.3°, respectively. The two aromatic CH/ π hydrogen bonds with relative short interaction distance may hinder the rotation of the terminal phenyl ring of the distyrylbenzene segment effectively. In the crystal of *cis*-*m*-4FDP the aromatic CH/ π hydrogen bond (interaction **VI**) is formed between two adjacent molecules with interaction distance of 2.98 Å and C–H– π center angle of

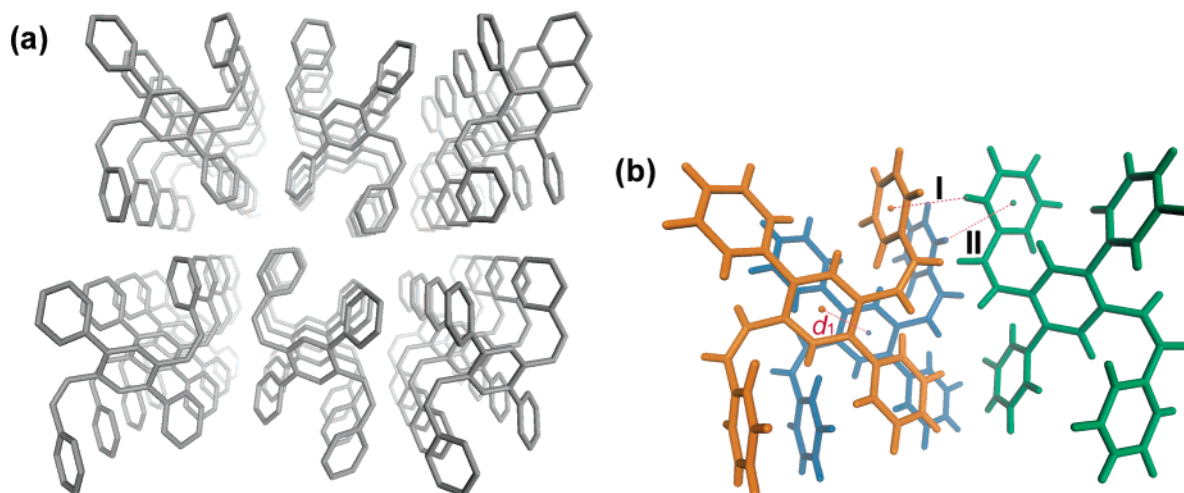


Figure 2. (a) Stacking images of *cis*-DPDSB. The hydrogen atoms have been omitted for clarity. (b) The schematic intermolecular interactions in the crystal of *cis*-DPDSB. The distance between two molecules within one column (d_1) is 5.49 Å. The interaction distance and the angle of C–H– π center for interaction I are 3.09 Å and 163.1°, and for interaction II they are 3.71 Å and 146.9°, respectively.

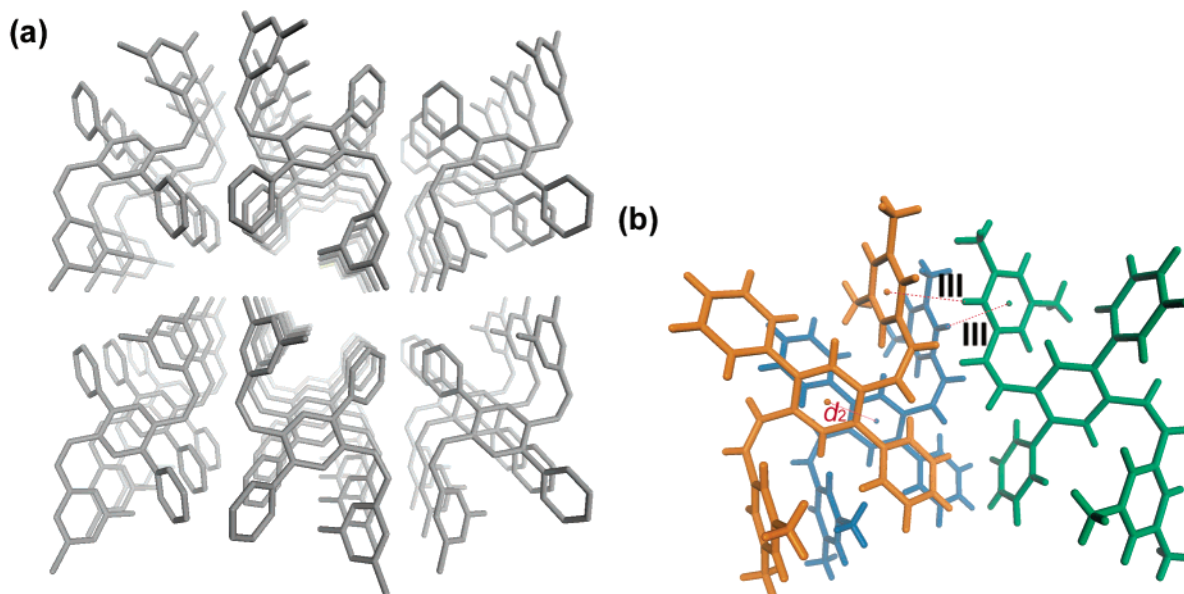


Figure 3. (a) Stacking images of *cis*-*m*-4MeDSB. The hydrogen atoms have been omitted for clarity. (b) The schematic intermolecular interactions in the crystal of *cis*-*m*-4MeDSB. The distance between two molecules within one column (d_2) is 5.68 Å. The interaction distance and the angle of C–H– π center for interaction III are 3.23 Å and 149.6°.

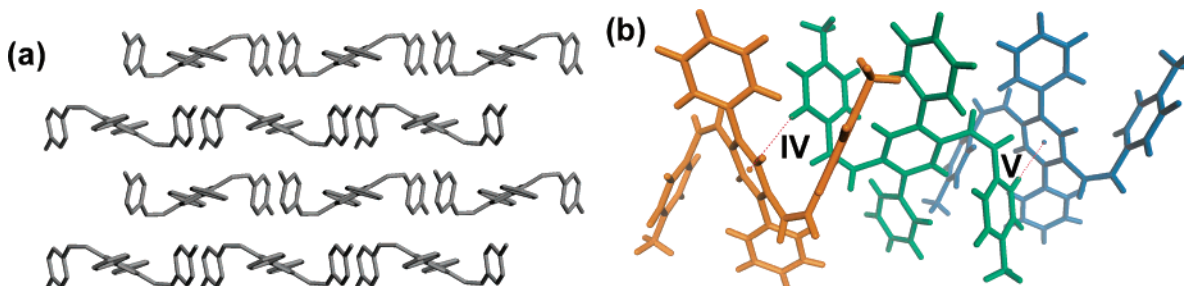


Figure 4. (a) “Brickwall motif” stacking image of *cis*-*p*-2MeDSB. The hydrogen atoms have been omitted for clarity. (b) The schematic intermolecular interactions in the crystal of *cis*-*p*-2MeDSB. The interaction distance and the angle of C–H– π center for interaction IV are 3.06 Å and 161.4°, and those for interaction V are 2.84 Å and 170.3°, respectively.

151.1°. For every *cis*-*m*-4FDP molecule, the terminal phenyl ring of the distyrylbenzene segment acts as an H donor and the terminal phenyl ring of the terphenyl segment acts as an H acceptor.

Although the backbones have relatively large torsional angles (Table 2, $\theta_{(1,2,3,4)}$, $\theta_{(2,3,4,5)}$, $\theta_{(3,4,5,6)}$), semiempirical calculations

showed that the transition dipole moments of the four *cis* compounds between the ground state and the first excited state are along the distyrylbenzene segments, which corresponds to the frontier molecular orbital distribution as we reported before.²² Then from the crystal stacking images, we can see that the dipole stacking modes for *cis*-DPDSB and *cis*-*m*-

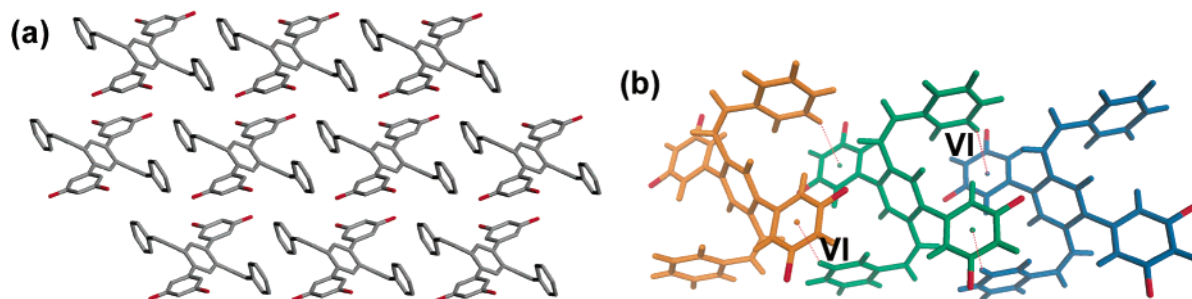


Figure 5. (a) Stacking images of *cis-m*-4FDP. The hydrogen atoms have been omitted for clarity. (b) The schematic intermolecular interactions in the crystal of *cis-m*-4FDP. The interaction distance and the angle of C—H \cdots π center for interaction VI are 2.98 Å and 151.1°.

TABLE 3: Summary of the Aromatic CH/ π Interactions in Four Crystals

| CH/ π interaction | distance of H \cdots ring (Å) | distance of C \cdots ring (Å) | angle of C—H \cdots ring (deg) |
|------------------------------------|---------------------------------|---------------------------------|----------------------------------|
| I | 3.09 | 3.99 | 163.1 |
| II (<i>cis</i> -DPDSB) | 3.71 ^a | 4.53 | 146.9 |
| III (<i>cis-m</i> -4MeDSB) | 3.23 | 4.09 | 149.6 |
| IV | 3.06 | 3.90 | 161.4 |
| V (<i>cis-p</i> -2MeDSB) | 2.84 | 3.76 | 170.3 |
| VI (<i>cis-m</i> -4FDP) | 2.98 | 3.88 | 151.1 |

^a The distance is too large to form a CH/ π interaction.

4MeDSB are parallel. Regarding the relatively large distance (5.49 and 5.68 Å), they cannot be regarded as *H*-aggregate; at least the interdipole interactions are very weak. For *cis-p*-2MeDSB and *cis-m*-4FDP the dipole stacking images are more like *J*-aggregate, though they are not typical and the interaction should be weak. For all four *cis* compounds, the weak interdipole interactions will decrease the aggregation quenching, not as in other planar molecular systems such as unsubstituted PPV and distyrylbenzene.²³ Actually, the single crystals of all

the *cis* compounds exhibit very intense blue emission when excited under an ultraviolet lamp (365 nm) as shown in the bottom of Figure 1. The fluorescence properties of the four *cis* compounds are discussed in the following section.

Photophysical Properties. The absorption spectra of the four *cis* compounds in THF are shown in Figure 6. For every *cis* compound, there are two main absorption bands: one located at about 320 nm that corresponds to the π -electron transition ($\pi \rightarrow \pi^*$) on the distyrylbenzene segment, and the other located at about 270 nm, attributed to the absorption of the *p*-terphenyl segment. When compared with the absorption spectrum of the *cis*-DPDSB, the intensity of the bands at about 320 nm of *cis-m*-4MeDSB and *cis-p*-2MeDSB is increased and has a small red shift (Table 4), which can be attributed to the electron-donating effect of the methyl groups. The absorption band at 270 nm of *cis-m*-4FDP increases obviously compared with the other three molecules, which comes from the positive mesomeric effect of the fluorine substituent.

The formation of the particles in the mixture of good solvent and poor solvent is easy to control by changing the ratios of

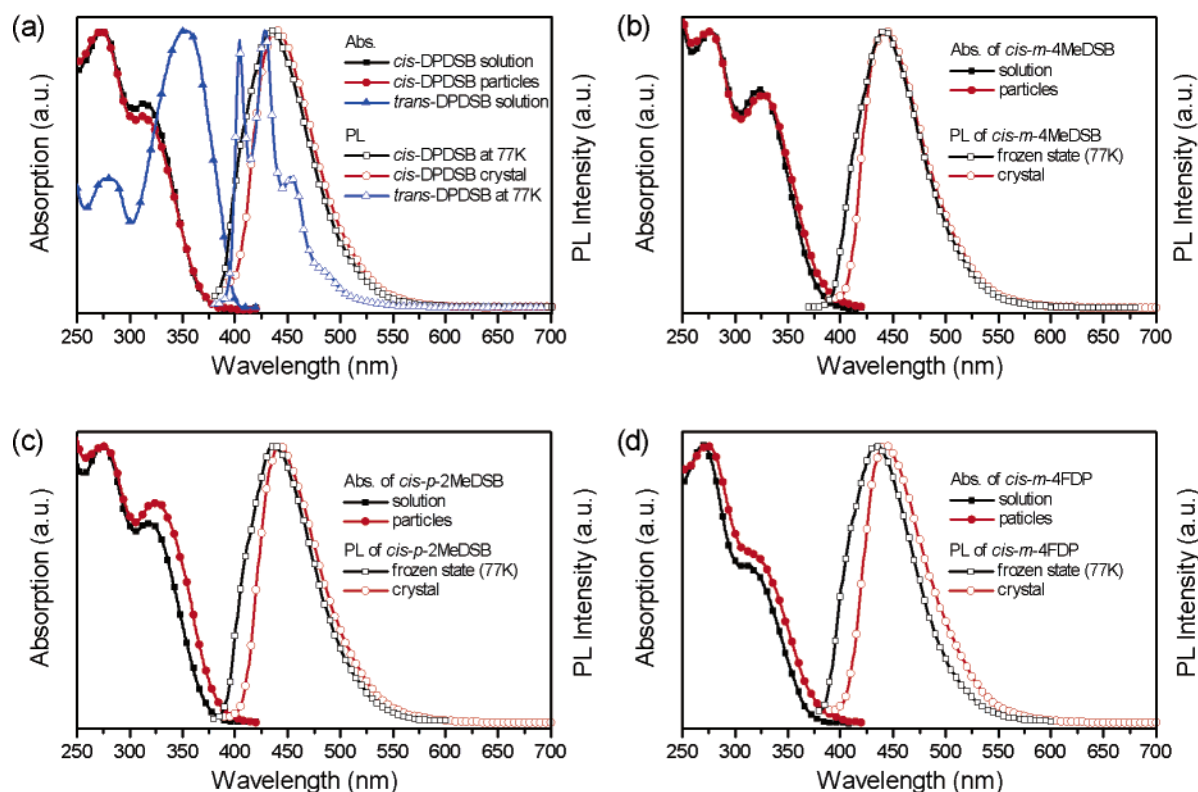


Figure 6. Absorption and PL spectra of the four *cis* compounds. Absorption and low-temperature PL of *trans*-DPDSB is also given in panel a for comparison. THF is used as solvent for solution absorption (3×10^{-5} mol L⁻¹) and a THF/water mixture is used for particles absorption (3×10^{-5} mol L⁻¹). CHCl₃ is used as solvent for low-temperature PL (5×10^{-6} mol L⁻¹). All the spectra are normalized.

TABLE 4: Optical Properties of Four Cis Compounds and trans-DPDSB

| material | abs in THF (nm) | PL (nm) | | PL efficiency in crystal |
|-------------------------------|-----------------|--------------------|---------|--------------------------|
| | | frozen glass state | crystal | |
| <i>cis</i> -DPDSB | 273, 315 | 435 | 439 | 0.36 |
| <i>cis</i> - <i>m</i> -4MeDSB | 277, 323 | 442 | 443 | 0.42 |
| <i>cis</i> - <i>p</i> -2MeDSB | 274, 318 | 438 | 442 | 0.51 |
| <i>cis</i> - <i>m</i> -4FDP | 270, 313 | 434 | 443 | 0.46 |
| <i>trans</i> -DPDSB | 277, 354 | 404, 428, 452 | | |

the solvents. At the beginning of the particle formation, the light scattering can be ignored because the size of the particles is much smaller than the length of the visible light. Then we try to record the absorption of the particles formed in THF (good solvent) and water (poor solvent) mixture. The particle absorption spectra of the four cis compounds are very similar to their absorption in dilute THF solutions, except for a small difference corresponding to the absorption bands at about 315 nm, such as a minor decrease in absorbance for *cis*-DPDSB (Figure 6a) and a small red shift together with a minor increase in absorbance for *cis*-*p*-2MeDSB (Figure 6c) and *cis*-*m*-4FDP (Figure 6d).

The *cis* isomer has almost no emission in molecularly dissolved solutions, due to the easy photochemical processes: *cis*-*trans* isomerization and photocyclization resulting from or together with intramolecular vibrational and rotational motions of the double bonds.¹⁶ To study the emission properties of the isolated molecules without photochemical processes, we have used the frozen dilute CHCl₃ solution at the 77 K glass state of the four *cis* compounds and recorded their PL spectra. All the *cis* compounds show very intense blue emission. Figure 6 shows the PL spectra of the four *cis* compounds in the frozen glass state. There is a small difference between different *cis* compounds in the frozen state, which comes from different substituents. The intense emission from the isolated *cis*-isomeric molecules indicates that such nonplanar conjugated molecules can also act as light emitters when the photochemical processes and the intramolecular motions are hindered effectively.

All the crystals of the four *cis* compounds show intense blue emission (Figure 1) and the PL spectra are shown in Figure 6. Every crystal emission spectrum of the four *cis* compounds has only one emission peak located around 440 nm with poor structure, which is very similar to that coming from the frozen glass state. There is more or less red shift from frozen isolated molecules to crystals corresponding to different stacking modes. As shown in Table 4, the crystalline state PL efficiency measured by using an integrating sphere is from 0.36 to 0.51. The PL efficiency of *cis*-*p*-2MeDSB (0.51) and *cis*-*m*-4FDP (0.46) is relatively higher than that of *cis*-DPDSB (0.36) and *cis*-*m*-4MeDSB (0.42). As we discussed above, *cis*-DPDSB and *cis*-*m*-4MeDSB are packed in parallel mode with relative weak intermolecular interactions (tabulated in Table 3), while *cis*-*p*-2MeDSB and *cis*-*m*-4FDP are packed in *J*-aggregation mode with relative strong intermolecular interactions. It is the difference in the stacking mode and the difference in the intermolecular interactions that causes different crystalline state PL efficiency for the four *cis* compounds.

The *cis* isomers have almost no emission in solution but intense emission in the crystalline state, which is the typical AIE phenomenon. The AIE properties can be clarified furthermore by the enhancement of the emission efficiency from the isolated molecules to the aggregate particles. For example, the PL efficiency of *cis*-*p*-2MeDSB (3×10^{-5} mol L⁻¹) in THF is less than 0.002, and the isolated molecules show very weak fluorescence up to 60% volume fractions of water addition. But

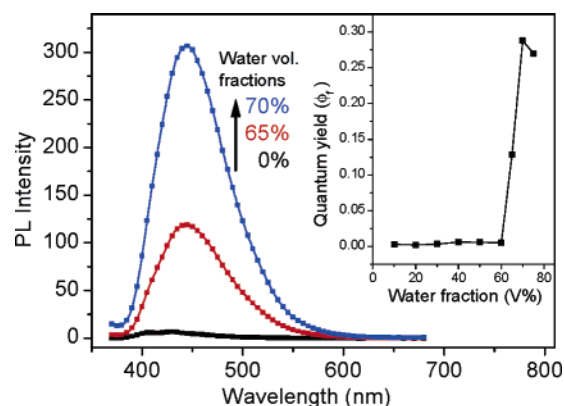


Figure 7. PL spectra of *cis*-*p*-2MeDSB (3×10^{-5} mol L⁻¹) in the different water/THF fraction solutions. The inset shows the change in the relative quantum yields (Φ_f) of *cis*-*p*-2MeDSB versus water fractions in THF.

at over 60% volume fractions of water added, when the molecules clustered to aggregate particles, the Φ_f values increase dramatically and have similar emission to that of the crystals. Figure 7 shows the PL spectra of *cis*-*p*-2MeDSB (3×10^{-5} mol L⁻¹) in the different water/THF fractions solutions and the PL efficiency versus different water/THF fractions. This enhanced emission by poor solvent is a common phenomenon in AIE active materials, and has been reported in several systems.^{6,10,12,13,15}

As discussed above, the emission spectra from all the crystals of four *cis* compounds are very similar, despite the different stacking images for different compounds. These similar emissions from different stacking modes mean that the luminescence does not come from the aggregated molecular clusters or excimer (a common phenomenon in the aggregate state). As shown in Figure 6, for every *cis* compound the red shift from isolated molecules (frozen glass state) to the crystals is from 1 to 9 nm. The minor difference between the isolated molecules and the crystals proves that the isolated molecules act as the emitting species in the crystals. The molecular stacking modes have a minor effect on the luminescence properties. In other words, such types of nonplanar molecules can effectively decrease the interdipole interactions by increasing the intermolecular distance. This weak interdipole interaction together with the intermolecular interactions induced stabilized excited state in crystals makes all four *cis* compounds have relatively high solid-state PL efficiency. The results indicate that we can realize high efficiency AIE through a decrease in the interdipole interactions by molecular modification.

The fact that the different stacking modes of the four *cis* compounds have a minor effect on the optical properties can be testified by the small difference between the isolated molecules absorption and the solid-state absorption. The small decrease in absorbance of *cis*-DPDSB from isolated molecules to particles comes from the weak parallel interdipole interactions. As for *cis*-*m*-4MeDSB there is almost no difference between the absorption in dilute THF solutions and particles due to the increased interdipole distance, while for *cis*-*p*-2MeDSB and *cis*-*m*-4FDP, the particles absorption corresponding to the distyrylbenzene segment has small red shifts and the absorption intensity increased, which may come from the weak interdipole interactions of *J*-aggregation.

The Essential Emission Properties of the Cis Isomers. When we compare the emission properties of *cis*-DPDSB and *trans*-DPDSB (Figure 6a), the most obvious feature is that the PL spectrum of *cis*-DPDSB has only one emission peak with

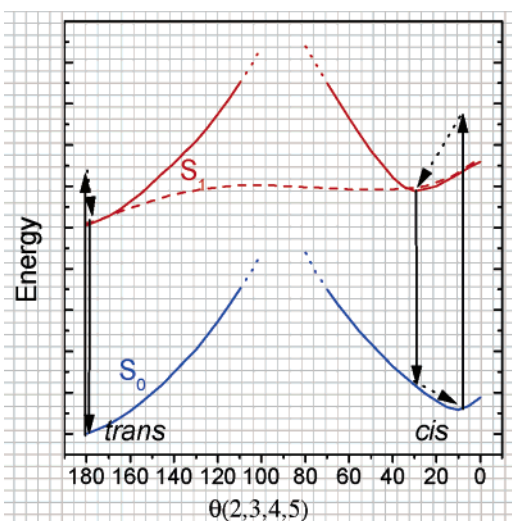


Figure 8. Schematic of the energy levels of the ground state (S_0) and the first singlet-excited state (S_1) of free isolate molecule, and the red solid line represents S_1 of the forbidden molecule (crystalline state or frozen state).

poor structure, not like *trans*-DPDSB having several fine emission bands. The second feature is the emission energy of *cis*-DPDSB is somewhat more red-shifted than *trans*-DPDSB, which seems opposite to the fact that the effective conjugation length of the trans isomer (planar backbone) is larger than that of the cis isomer (torsional backbone). The third feature is the cis isomers have a very large Stokes shift of about 120 nm with very small overlap between the absorption and emission bands. The reason for the poor structure and red-shifted PL spectra of the cis isomers can be tentatively explained by the energy levels shown in Figure 8.

As shown in Figure 8, on the first singlet-excited state (S_1) for the free isolate molecule there is almost no energy barrier from cis isomer to trans isomer, which is due to the elongated C—C bond (like single C—C bond) with easier rotation, while in the crystalline state (or frozen state), the energy barrier increased dramatically because of the interactions between the adjacent molecules (or from the frozen solvent molecules). It is well-known that as the isolated cis isomer is excited to the excited state, $\theta_{(2,3,4,5)}$ (the torsional angle of the double bond and its adjacent atoms) can increase up to 90° ,²⁴ then the isomerization to the trans isomer can occur very easily, which is also the reason the cis isomer shows almost no emission in solution. The easy isomerization of the isolated molecules at the first singlet excited state (S_1) can be attributed to the very low energy barrier from the cis isomer to the trans isomer as shown in Figure 8 (red dashed line),²⁵ while in the crystalline or the frozen glass state, the relatively rigid molecules induced by very rigid media ensure the intense emission from the cis isomer. At the ground state $\theta_{(2,3,4,5)}$ is about $6\text{--}9^\circ$ as discussed in the molecular structure section. The moment the molecule is excited, it maintains the configuration of the ground state according to Franck–Condon principle. But in the excited state the length of the double bond will be increased and then this bond is more like a single bond, which makes the rotation around this bond easier. The values of $\theta_{(2,3,4,5)}$, $\theta_{(1,2,3,4)}$, and $\theta_{(3,4,5,6)}$ become averaged and this relaxation process occurs during the transition of molecular relaxation to the lowest vibrational excited state. When the excited molecule transfers to the ground state, it maintains the configuration of the excited state, different from the ground state. And then the ground state molecule with relatively higher vibration energy level (large

value of $\theta_{(2,3,4,5)}$) can relax to the lowest vibration energy level ($\theta_{(2,3,4,5)} < 10^\circ$). It is the configuration difference between the ground state and the excited state that induces a very large Stokes shift for the cis isomer. For the trans isomer, the rigidity of the backbone diminishes the configuration difference between the ground state and the excited state, and the rigid backbone ensures the molecule has clear ground-state vibration energy levels that can correspond to the several emission bands in the PL spectrum. The emission spectrum from the poor structure of the cis-isomer comes from the abundant vibration energy levels of the torsional molecule with changeable configuration.

Conclusion

cis-DPDSB and its derivatives are a class of nonplanar conjugated compounds. This class of materials has almost no emission in solution but intense emission in crystal, which is a typical AIE property. The interdipole interactions in crystal become very weak because of the increased intermolecular distance, which enables different stacking modes to have a minor effect on the optical properties. The isolated molecules of the cis isomer can act as efficient light emitters when the intramolecular motions such as isomerization of the double bonds and torsional vibration of the substituted phenyl group are hindered effectively, using frozen-state solution or crystal. The different crystalline state PL efficiency for the four cis compounds comes from the different stacking modes and intermolecular interactions present in their crystalline state. There is a very large Stokes shift of this class of nonplanar compounds, which comes from the relatively large configuration difference between the ground state and the first singlet excited state. The abundant vibration energy levels of the torsional molecule with changeable configuration enable the emission spectrum to have only one broad emission band with poor structure.

Acknowledgment. We thank Professor Heinz Bässler very much for his helpful suggestions, and are grateful for financial support from the National Science Foundation of China (grant nos. 20573040, 20474024, 20125421, 90101026, and 50473001), Ministry of Science and Technology of China (grant no. 2002CB6134003), and PCSIRT.

Supporting Information Available: Synthesis and characterization of *cis-m*-4MeDSB, *cis-p*-2MeDSB, and *cis-m*-4FDP and X-ray crystallographic information files (CIF file) for the four cis compounds. This material is available free of charge via the Internet at <http://pubs.acs.org>.

References and Notes

- (1) (a) Friend, R. H.; Gymer, R. W.; Holmes, A. B.; Burroughes, J. H.; Marks, R. N.; Taliani, C.; Bradley, D. D. C.; Dos Santos, D. A.; Bredas, J. L.; Logdlund, M.; Salaneck, W. R. *Nature* **1999**, *397*, 121. (b) Jenekhe, S. A.; Osaheni, J. A. *Science* **1994**, *265*, 765.
- (2) Provier, T.; Urban, M. W. *Film Formation in Coatings: Mechanisms, Properties, and Morphology*; American Chemical Society: Washington, DC, 2001.
- (3) Luo, J.; Xie, Z.; Lam, J. W. Y.; Cheng, L.; Chen, H.; Qiu, C.; Kwok, H. S.; Zhan, X.; Liu, Y.; Zhu, D.; Tang, B. Z. *Chem. Commun.* **2001**, 1740.
- (4) Chen, J.; Xu, B.; Yang, K.; Cao, Y.; Sung, H. H. Y.; Williams, I. D.; Tang, B. Z. *J. Phys. Chem. B* **2005**, *109*, 17086.
- (5) (a) Chen, J.; Xie, Z.; Lam, J. W. Y.; Law, C. C. W.; Tang, B. Z. *Macromolecules* **2003**, *36*, 1108. (b) Wang, F.; Luo, J.; Chen, J.; Huang, F.; Cao, Y. *Polymer* **2005**, *46*, 8422.
- (6) Chen, J.; Law, C. C. W.; Lam, J. W. Y.; Dong, Y.; Lo, S. M. F.; Williams, I. D.; Zhu, D.; Tang, B. Z. *Chem. Mater.* **2003**, *15*, 1535.
- (7) Li, Z.; Dong, Y.; Mi, B.; Tang, Y.; Halussler, M.; Tong, H.; Dong, Y.; Lam, J. W. Y.; Ren, Y.; Sung, H. H. Y.; Wong, K. S.; Gao, P.; Williams, I. D.; Kwok, H. S.; Tang, B. Z. *J. Phys. Chem. B* **2005**, *109*, 10061.

- (8) Ren, Y.; Dong, Y.; Lam, J. W. Y.; Tang, B. Z.; Wong, K. S. *Chem. Phys. Lett.* **2005**, *402*, 468.
- (9) (a) Yu, G.; Yin, S.; Liu, Y.; Chen, J.; Xu, X.; Sun, X.; Ma, D.; Zhan, X.; Peng, Q.; Shuai, Z.; Tang, B. Z.; Zhu, D.; Fang, W.; Luo, Y. *J. Am. Chem. Soc.* **2005**, *127*, 6335. (b) Yin, S.; Peng, Q.; Shuai, Z.; Fang, W.; Wang, Y. H.; Luo, Y. *Phys. Rev. B* **2006**, *73*, 205409.
- (10) (a) An, B. K.; Kwon, S. K.; Jung, S. D.; Park, S. Y. *J. Am. Chem. Soc.* **2002**, *124*, 14410. (b) Lim, S. J.; An, B. K.; Park, S. Y. *Macromolecules* **2005**, *38*, 6236. (c) Lim, S. J.; An, B. K.; Jung, S. D.; Chung, M. A.; Park, S. Y. *Angew. Chem., Int. Edit.* **2004**, *43*, 6346.
- (11) Yeh, H. C.; Yeh, S. J.; Chen, C. T. *Chem. Commun.* **2003**, 2632.
- (12) Bhongale, C. J.; Chang, C. W.; Lee, C. S.; Diau, W. G.; Hsu, C. S. *J. Phys. Chem. B* **2005**, *109*, 13472.
- (13) Chen, J.; Xu, B.; Ouyang, X.; Tang, B. Z.; Cao, Y. *J. Phys. Chem. A* **2004**, *108*, 7522.
- (14) (a) Deans, R.; Kim, J.; Machacek, M. R.; Swager, T. M. *J. Am. Chem. Soc.* **2000**, *122*, 8565. (b) Belton, C.; O'Brien, D. F.; Blau, W. J.; Cadby, A. J.; Lane, P. A.; Bradley, D. D. C.; Byrne, H. J.; Stockman, R.; Hörhold, H. H. *Appl. Phys. Lett.* **2001**, *78*, 1059. (c) Holzer, W.; Penzkofer, A.; Stockmann, R.; Meysel, H.; Liebegott, H.; Hörhold, H. H. *Polymer* **2001**, *42*, 3183.
- (15) Wang, Z.; Shao, H.; Ye, J.; Tang, L.; Lu, P. *J. Phys. Chem. B* **2005**, *109*, 19627.
- (16) Xie, Z.; Yang, B.; Cheng, G.; Liu, L.; He, F.; Shen, F.; Ma, Y.; Liu, S. *Chem. Mater.* **2005**, *17*, 1287.
- (17) (a) Wong, K. F.; Skaf, M. S.; Yang, C. Y.; Rossky, P. J.; Bagchi, B.; Hu, D.; Yu, J.; Barbara, P. F. *J. Phys. Chem. B* **2001**, *105*, 6103. (b) Chen, Y. S.; Meng, H. F. *Phys. Rev. B* **2002**, *66*, 035202. (c) Summers, M. A.; Kemper, P. R.; Bushnell, J. E.; Robinson, M. R.; Bazan, G. C.; Bowers, M. T.; Buratto, S. K. *J. Am. Chem. Soc.* **2003**, *125*, 5199. (d) Claudio, G. C.; Bittner, E. R. *J. Chem. Phys.* **2001**, *115*, 9585.
- (18) (a) Müllen, K.; Wegner, G. *Electronic Materials: The Oligomer Approach*; Wiley VCH: Weinheim, Germany, 1998. (b) Xie, Z.; Yang, B.; Li, F.; Cheng, G.; Liu, L.; Yang, G.; Xu, H.; Ye, L.; Hanif, M.; Liu, S.; Ma, D.; Ma, Y. *J. Am. Chem. Soc.* **2005**, *127*, 14152.
- (19) *SHELXTL Reference Manual*, version 5.1; Bruker AXS Inc.: Madison, WI, 1998.
- (20) Xie, Z.; Liu, L.; Yang, B.; Yang, G.; Ye, L.; Li, M.; Ma, Y. *Cryst. Growth Des.* **2005**, *5*, 1959.
- (21) Feast, W. J.; Lövenich, P. W.; Puschmann, H.; Taliani, C. *Chem. Commun.* **2001**, 505.
- (22) Xie, Z.; Yang, B.; Liu, L.; Li, M.; Lin, D.; Ma, Y.; Cheng, G.; Liu, S. *J. Phys. Org. Chem.* **2005**, *18*, 962.
- (23) (a) van Hutten, P. F.; Wildeman, J.; Meetsma, A.; Hadziioannou, G. *J. Am. Chem. Soc.* **1999**, *121*, 5910. (b) Wu, C. C.; DeLong, M. C.; Vardeny, Z. V.; Ferraris, J. P. *Synth. Met.* **2003**, *137*, 939.
- (24) Jiang Y.; Li, T. *Photo Chemistry*; Chemical Industry Press: Beijing, China, 2005.
- (25) Han, W. G.; Lovell, T.; Liu, T.; Noodleman, L. *ChemPhysChem* **2002**, *3*, 167.